

MODELLING THE HEATING AND EROSION OF A NON-REFRACTORY CATHODE IN A PLASMA TORCH

A. MONNOYER*, P. FRETON, J.-J. GONZALEZ

Laplace, UMR 5213 CNRS-UPS-INP, Université Paul Sabatier, 118 route de Narbonne, 31062 Toulouse, France

* monnoyer@laplace.univ-tlse.fr

Abstract. In this work, we study the heating of a hollow cylindrical copper electrode subjected to a rotating arc root modeled by a moving heat flux profile. The problem is solved analytically using a two time scale analysis. In accordance with previous literature works, it is shown that, whenever using reasonable values for the heat flux below the arc root, the fusion temperature of the material is not reached. We explain the experimentally evidenced erosion by the existence within the arc root, at smaller length scales, of cathode microspots. The cathode spot model presented in this paper gives orders of magnitude for the erosion rate in agreement with experiments.

Keywords: plasma torch, electric arc, copper cathode, heat conduction, erosion rate, cathode spots.

1. Introduction

Hollow cathode plasma torches have many applications in waste treatment or for simulating atmospheric re-entry conditions [1]. The peculiarity of these torches is the geometry of the cathode, which is the whole internal surface of a hollow cylinder, and that of the injection chamber, designed to generate a vortex flow. Around the cathode cylinder, a coil generates a (mostly axial) external magnetic field to rotate the arc root. The competition between the gasdynamic "forces" (mostly from the vortex flow) and magnetic forces acting on the arc results in a permanent regime in which the arc root rotates approximately in a plane at constant angular velocity (see Fig 1). We refer to works [2, 3] for a more detailed analysis of the arc behavior in this kind of plasma torch.

The arc root rotation is necessary to limit the exposure time of the cathode to the arc, and spread the erosion over a wider area to increase the technology's lifetime. The cathode is also cooled down on its external face by a water circulation to lower its temperature. Despite these precautions, the copper cathode erosion is still a strong limitation to the use of this technology. It is therefore important to better understand this erosion to be able to predict it, and if possible, to lower it.

In the important experimental work [4], it was shown that the mechanism of erosion is "simply" the fusion and vaporization of the cathode material. Previous literature works [5–7] have therefore attempted to evaluate the temperature field in the material to confirm this mechanism from a theoretical point of view. In these works, the cathode heating is typically represented by heat flux profiles derived from experiments such as [8, 9]. Unfortunately, all these works have concluded that the maximal temperature

reached on the cathode surface may remain below the fusion point while erosion is still observed experimentally. An explanation often proposed in the literature [6, 10, 11] is that the real arc root is made up of several very hot cathode (micro-)spots, in which the erosion occurs, and whose behavior is typically averaged out in experiments. Therefore, these cathode spots should somehow be included in the model to test this hypothesis, which is the main goal of this paper.

As a first step, the temperature field resulting from the magnetically displaced arc root is obtained, using "macroscopic" heat flux profiles (i.e. with cathode spots averaged out) derived from experiments made on an analogous system [8]. In the light of previous works [5–7], it is to be expected that fusion temperature may not be reached. Restricting ourselves to this problematic case, a purely analytical approach to the calculation of the macroscopic temperature field will be presented. This approach takes advantage of a strong ordering between the fast arc root rotation and the slow arc root streak cooling. Localized heating below the arc root is represented in a manner similar to [12]. Cathode spots will then be superposed to this macroscopic temperature field. They will be treated by a non-linear surface heating model involving a plasma layer close to the cathode [13]. This model was originally developed for vacuum arcs, so, its application to atmospheric pressure will be discussed.

The outline of the paper is as follows. In Section 2, the cathode heating model is presented, first from a macroscopic point of view, and then with account of cathode spots. Numerical results are presented and discussed in Section 3 and our main conclusions are summarized in Section 4.

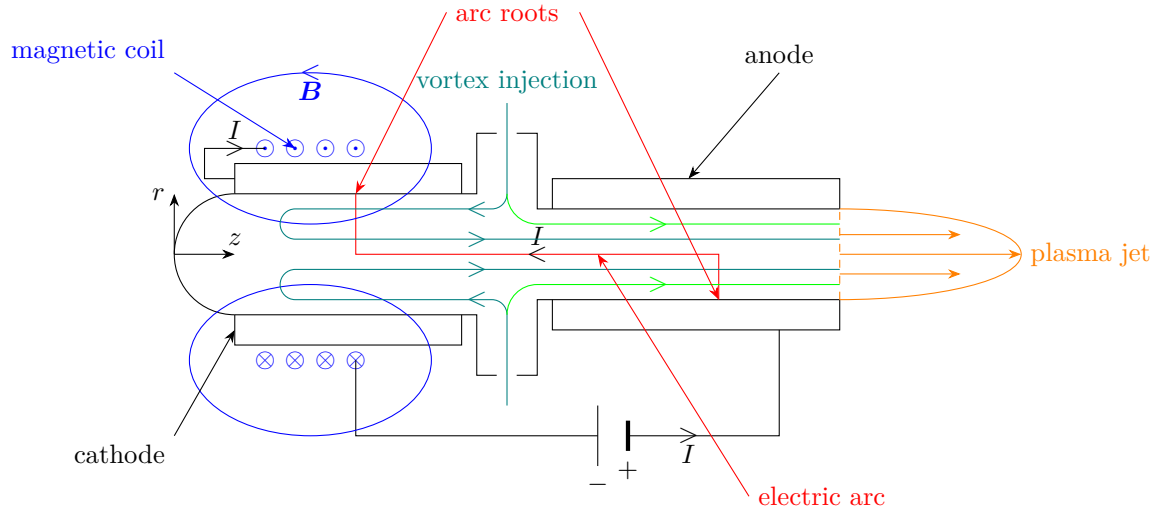


Figure 1. Working principle of hollow cathode plasma torches, with current I and external magnetic field \mathbf{B} .

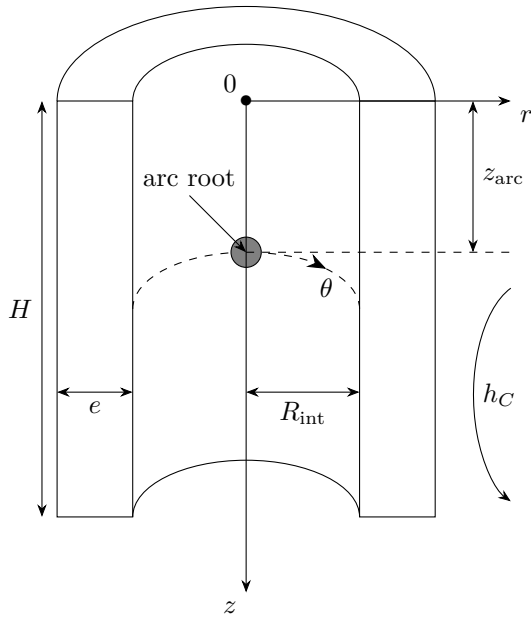


Figure 2. Sketch of the arc root trajectory

where D is the diffusivity of the material. The internal face is subject to the following boundary condition :

$$-\kappa \frac{\partial T}{\partial r}(R_{\text{int}}, \theta, z, t) = q_{\text{PA}}(d(\theta, z, t)), \quad (2)$$

where :

$$d(\theta, z, t) = \sqrt{(z - z_{\text{arc}})^2 + R_{\text{int}}^2(\theta - \omega t)^2}, \quad (3)$$

$$q_{\text{PA}}(d) = q_{\text{max}} \exp\left(-\frac{d^2}{r_s^2}\right),$$

where ω , q_{max} , and r_s are given parameters. This boundary condition describes the heating of the internal surface by a gaussian distributed arc root, whose center moves on a circle at $z = z_{\text{arc}}$ and at constant angular velocity ω . This trajectory is schematically represented in Figure 2.

Note that r_s may be interpreted as the arc root radius, since the total power of the source is the same as if the heat flux had the value q_{max} in the disc of radius r_s , as shown by the following calculation :

$$P_{\text{dep}} = 2\pi \int_0^\infty q_{\text{PA}}(r) r dr = q_{\text{max}} \pi r_s^2. \quad (4)$$

The external cylindrical surface is cooled down according to Newton's law of conducto-convection :

$$-\kappa \frac{\partial T}{\partial r}(R_{\text{ext}}, \theta, z, t) = h_C(T(R_{\text{ext}}, \theta, z, t) - T_{\text{fl}}), \quad (5)$$

where h_C (heat transfer coefficient) and T_{fl} (fluid temperature far from the thermal boundary layer) are given parameters.

Of course, this model does not describe some phenomena which may be of importance, such as phase changes or surface radiation losses. Therefore, the consistency of results with the model hypotheses should be verified in the end.

2. Theoretical model

2.1. Description of the heating problem

The hollow cathode heating problem under consideration is similar to that described in [5–7, 12]. It may be briefly presented as follows. The hollow cathode is modelled by a hollow cylinder of internal radius R_{int} , external radius R_{ext} , (its thickness is therefore $e = R_{\text{ext}} - R_{\text{int}}$) and height H . The system is naturally described in cylindrical coordinates (r, θ, z) (see Fig. 2).

In this geometry, we shall solve the unsteady heat conduction equation for temperature T , assuming uniform thermal conductivity κ , specific heat c_p and mass density ρ_m :

$$\frac{\partial T}{\partial t} = D \Delta T, \quad D = \frac{\kappa}{\rho_m c_p}, \quad (1)$$

2.2. Time scales of the problem

Using dimensional analysis, numerous time scales may be derived from parameters introduced in the model. Estimating these time scales may reveal strong orderings which would help simplifying the problem. The most relevant time scales and their typical numerical values are presented in Table 1.

To obtain numerical estimates, we have used the following values of parameters : $\kappa = 401 \text{ W/(m}\cdot\text{K)}$, $c_p = 385 \text{ J/(kg}\cdot\text{K)}$, $\rho_m = 8960 \text{ kg/m}^3$ (typical for a copper cathode), $r_s = 0.2 \text{ mm}$ (deduced from experiments [8]), $e = 1 \text{ cm}$, and $h_C = 30 \text{ kW/(m}^2\cdot\text{K)}$ (typical value of the heat transfer coefficient imposed by the water cooling circuit). The rotation period t_{arc} and exposure time are calculated for $v_{\text{arc}} = 100 \text{ m/s}$ and $R_{\text{int}} = 1.6 \text{ cm}$ which again, are typical values (see e.g. [3, 5]). The values reported in Table 1 reveal the following strong orderings :

$$\delta t \ll t_0 \ll t_{\text{arc}} \ll t_{\text{diff}} \sim t_{\text{cool}} \ll t_{\text{op}}. \quad (6)$$

These results indicate that the temperature field in the cathode will result from various heat conduction phenomena happening at different time scales. For example, while working at very long time scales t_{op} , it is legitimate to consider that the inner cathode surface receives the average heat flux profile :

$$\langle q_{\text{PA}} \rangle(z) = \frac{q_{\text{max}} r_s}{2\sqrt{\pi} R_{\text{int}}} \exp\left(-\frac{(z - z_{\text{arc}})^2}{r_s^2}\right), \quad (7)$$

which does not depend on θ . The solution to this averaged problem will give us an average temperature field $\langle T \rangle$ which corresponds to the average temperature in the arc root streak. It is nevertheless necessary to estimate the temperature increment δT just below the arc root since a significant localized heating exists at that place. For that purpose, we shall consider that any phenomenon happening at time scales slower than t_0 are frozen, which can be seen as an adiabatic approximation. With these hypotheses, the problem of evaluating δT may be reduced to the already worked out problem of a gaussian flux profile heating a semi-infinite bulk while moving at constant velocity at its surface.

2.3. Averaged solution

To derive the average solution, it is convenient to replace the Gaussian heat flux profile (7) by a Lorentzian profile with the same characteristics :

$$q_L(z) = \frac{P_{\text{lin}} d_S}{d_S^2 + (z - z_{\text{arc}})^2}, \quad (8)$$

$$P_{\text{lin}} = \frac{q_{\text{max}} r_s^2}{R_{\text{int}}}, \quad d_S = 2\sqrt{\pi} r_s.$$

Geometrically, this amounts to replacing condition (7) by a "heating wire" with power per unit length P_{lin}

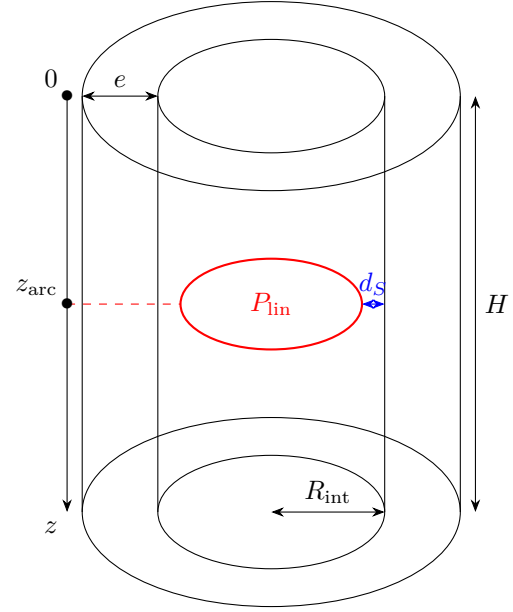


Figure 3. Representation of averaged heating by a line power source

at distance d_S from the inner surface, as illustrated in Fig 3.

Moreover, if we consider the case of a thin electrode, that is $e \ll R_{\text{int}}$, then we may approximate the isothermal surfaces by toric surfaces. In this case, the heat flux inside the cathode may be written :

$$\mathbf{q} = \frac{P_{\text{lin}} \boldsymbol{\rho}}{2\pi \rho^2}, \quad \boldsymbol{\rho} = (z - z_{\text{arc}}) \mathbf{e}_z + K \mathbf{e}_r, \quad (9)$$

where $K = r - R_{\text{int}} + d_S$. The relation $\nabla \cdot \mathbf{q} = 0$ is easily verified in the limit $e \ll R_{\text{int}}$, in which case we have $K \ll r$. Integrating this equation using Fourier's law, as well as the boundary conditions, we obtain the averaged temperature field :

$$\langle T \rangle = T_{\text{fl}} + \frac{P_{\text{lin}}}{2\pi(d_S + e)h_C} + \frac{P_{\text{lin}}}{2\pi\kappa} \ln\left(\frac{d_S + e}{\rho}\right), \quad (10)$$

which may be evaluated at $\rho = d_S$ (i.e. $r = R_{\text{int}}$ and $z = z_{\text{arc}}$) to obtain the maximal value of $\langle T \rangle$.

2.4. Solution below the arc root

Let us now assume that the average field $\langle T \rangle$ obtained in the Sec. 2.3 is established. We shall now derive the temperature field just below the moving arc root. The penetration depth of the temperature field $\sqrt{D\delta t}$ is much smaller than the cathode thickness, and the arc root radius r_s is much smaller than the cathode inner radius R_{int} . We may therefore represent heat conduction below the arc root by that of a gaussian spot moving at constant velocity $v = R_{\text{int}}\omega$ on the cathode surface, considered as a cartesian semi-infinite medium. The solution to this problem has already been worked out (see e.g. [14], p 73 or [12]) and may be written :

Time scale	Notation and definition	Typical value
Long conduction time	$t_{\text{diff}} = e^2/D$	0.86 s
Short conduction time	$t_0 = r_s^2/4D$	88 μs
Cooling time	$t_{\text{cool}} = \rho_m c_p e/h_C$	1.15 s
Arc root rotation period	$t_{\text{arc}} = 2\pi R_{\text{int}}/v_{\text{arc}}$	1 ms
Exposure time	$\delta t = 2r_s/v_{\text{arc}}$	4 μs
Operation time	t_{op}	1 h

Table 1. Time scales of the heat conduction problem

$$T(x, y, z, t) = T_0 + \frac{2P_{\text{dep}}}{(4\pi D)^{3/2} \rho_m c_p} \int_0^t \frac{dt'}{\sqrt{t'(t_0 + t')}} \exp\left(-\frac{z^2}{4Dt'} - \frac{x^2 + y^2}{4D(t_0 + t')}\right) - \frac{vx}{2D} \frac{t - t'}{t' + t_0} - \frac{v^2}{4D} \frac{(t - t')^2}{t' + t_0} \Bigg) . \quad (11)$$

This integral may easily be calculated numerically (see Section 3.1).

2.5. Account of cathode microspots

In this work, the cathode spots were modelled using a non-linear surface heating approach imposed by the physics of a near-cathode plasma layer (NCPL). This approach was mainly developed for refractory cathodes working in a high-pressure (i.e. ≥ 1 bar) plasma, a typical example being the argon-tungsten system (see e.g. review [15] and references therein). This approach was also developed for non-refractory cathodes in the case of the so-called "vacuum" arc, particularly in works [13, 16]. It seems reasonable to apply these last works to our case, adopting the following hypotheses :

- The atmospheric pressure is assumed to play a minor role on the cathode spot structure and properties : this hypothesis is reasonable since vapor pressures generated by the spot is highly above atmospheric.
- The spots are treated as quasi-stationary, the underlying assumption being that their lifetime is much larger than their ignition time.

We have thus independently re-developed the NCPL model for vacuum arcs [13]. The most important results delivered by this model are the electrical, thermal, and erosion characteristics of the cathode layer, which give the current density j , the heat flux density q , and the mass flux density g as functions of a given sheath voltage U and the local temperature T_w , and we shall denote them by $j(T_w, U)$, $q(T_w, U)$, and $g(T_w, U)$.

The characteristics of a single spot are then obtained employing an approach similar to that described in [17]. A cathode spot within the arc root is then modelled by a disc of radius r_s , in which the temperature

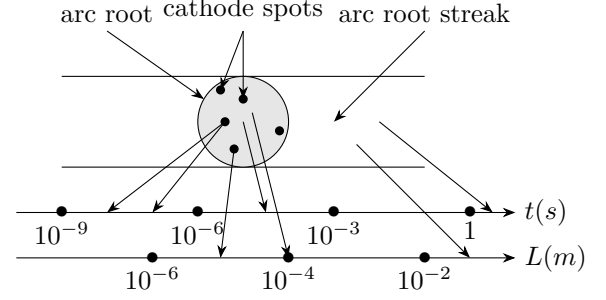


Figure 4. Summary of the structures considered and associated time and length scales

T_s is uniform, at the surface of a semi-infinite material with a background temperature $T_0 < T_s$. The originality of our approach resides in the choice of this temperature as $T_0 = \langle T \rangle + \delta T$. In other words, we superpose the spots on the more macroscopic arc root, as illustrated in Fig 4.

The temperature T_s may be arbitrarily given as corresponding to the maximal heat flux $q(T, U)$ for a given U , as was done in [17]. The spot radius r_s is then determined by an equation of integral heat balance, i.e. :

$$q(T_s, U) \pi r_s^2 = 4r_s \int_{T_0}^{T_s} \kappa(T) dT, \quad (12)$$

$$\implies r_s = \frac{4}{\pi q(T_s, U)} \int_{T_0}^{T_s} \kappa(T) dT.$$

Note that our approach of evaluating r_s is different from that employed in [17]. Once r_s and T_s have been determined (or chosen), we may then obtain the characteristics of a single spot for a given voltage drop U and in particular, the current per spot $I_s = j(T_s, U) \pi r_s^2$ and the erosion rate per spot $G = g(T_s, U) \pi r_s^2$. Knowing the total current I , we may evaluate the number of spots as $N_s = I/I_s$. Alternatively, we may obtain the voltage drop U for a given number of spots N_s , which ensures this number will always be an integer.

3. Results and discussion

3.1. Results of the heating model

The average temperature $\langle T \rangle$ in the arc root streak is readily evaluated from Eq 10. Using typical param-

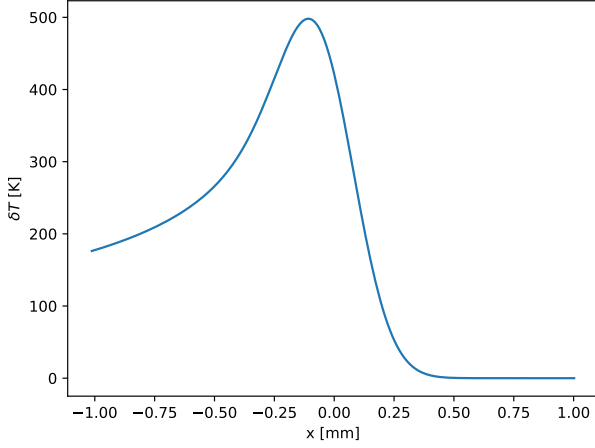


Figure 5. Temperature increment below the moving arc root.

ters discussed above, as well as $T_{fl} = 300$ K, we find $\langle T \rangle = 362$ K. This value is far below the fusion point of copper (1350 K), which should not surprise since localized heating below the arc root is not yet considered. This value is also consistent with the hypotheses of the model described in Sec 2.1.

For a numerical calculation of integral 11, it is easier to express the solution in the reference frame defined by $x' = x - v(t + t_0)$. Since we are working at time scales much larger than t_0 , we may set for definiteness $t = 10t_0$ and calculate the integral by the trapezoidal rule. The change of variable $t' = u^2$ was also performed to remove the (apparent) singularity at the origin of time. The temperature field on the cathode surface along direction x (i.e. $T(x, 0, 0, 10t_0)$) is represented in Figure 5, in the reference frame of the moving spot. The maximal value corresponds to the sought increment δT and is equal to 498 K.

The temperature below the arc root is evaluated by summing contributions $\langle T \rangle$ and δT , which gives a result of 860 K. This temperature is still significantly below the fusion point of the copper material. This result is in contradiction with experiments : it is well known that copper cathodes of plasma torches undergo a significant erosion due to melting and/or vaporization of the electrode. This conclusion is similar to that obtained in previous works [5–7].

3.2. Erosion rate according to the cathode spot model

An example of $j(T_w, U)$, $q(T_w, U)$ and $g(T_w, U)$ functions is given in Fig. 6 for $U = 20$ V. We refer to [13] for a detailed discussion of these functions. Here, we only mention that the drop in mass flux density at $T_w \sim 3900$ K is due to an increase of ionization of the vaporized atoms, which may therefore return to the surface as ions due to the potential profile at the vicinity of the cathode. This also explains why the heat flux q increases at this temperature, since this heating is mostly due to ionic bombardment.

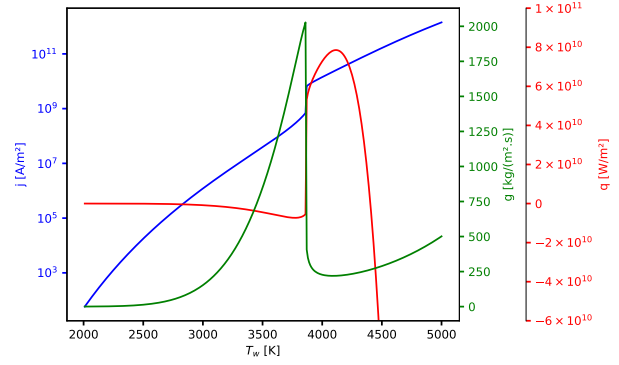


Figure 6. Heat and mass flux density imposed by the cathode layer physics as a function of surface temperature T_w . $U = 20$ V.

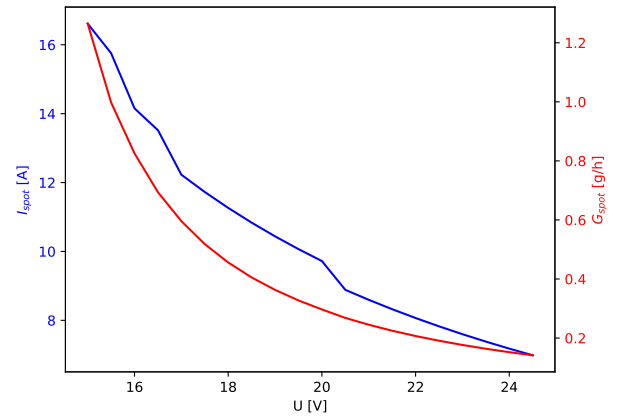


Figure 7. Total current and erosion rate for a single spot as a function of the sheath voltage. $T_0 = 860$ K

Applying the cathode spot model described in Section 2.5, we obtain the electrical and erosion characteristics represented in Figure 7 for a single spot.

For example, if we choose $U = 20$ V and $T_0 = 860$ K according to the macroscopic study, we obtain a current per spot of $I_s = 9.7$ A, and an erosion rate per spot of $G_s = 0.29$ g/h. Since we work at $I = 200$ A, the number of spots is approximately $N_s = 21$ and the total erosion rate is $G = N_s G_s = 6.1$ g/h. This order of magnitude is in good agreement with experimental erosion rates for cathodes of plasma torches working with such a current intensity, and with air as a plasma gas. It may easily be proven that, within the scope of the presented model, this global erosion rate does not depend on the macroscopic arc root temperature T_0 .

4. Conclusions

This work presented a model which may be useful for the prediction of temperature fields and erosion rates in hollow cathode plasma torches. The model's applicability is in fact not limited to this particular situation : it may in principle be applied in any situation where a moving arc root exists on a non-refractory cathode. The model seems to give good orders of magnitude for the erosion rate of copper cathodes

working with an air plasma at current intensities of a few hundred A. However, several important phenomena were not considered here and the predictions of the model may differ significantly from experimental results in other situations. For example, while valid for an air plasma the assumption of continuous arc root displacement may be inadequate in some plasma gases, as the nature of this movement (continuous or by successive jumps) depends on the thickness of the oxide layer (see [18]). However, further investigation on this point from the theoretical point of view is beyond the scope of this paper. Other sources of improvement include an account of Joule effect in the material and the emission of droplets, which may give a significant contribution to the total erosion.

References

- [1] M. F. Zhukov and I. M. Zasypkin. *Thermal plasma torches: design, characteristics, application*. Cambridge Int Science Publishing, 2007. ISBN 1-280-73876-6.
- [2] P. Freton, J.-J. Gonzalez, and G. Escalier. Prediction of the cathodic arc root behaviour in a hollow cathode thermal plasma torch. *Journal of Physics D: Applied Physics*, 42(19):195205, 2009. doi:10.1088/0022-3727/42/19/195205.
- [3] F. Sambou, J. J. Gonzalez, M. Benmouffok, and P. Freton. Theoretical study of the arc motion in the hollow cathode of a dc thermal plasma torch. *Journal of Physics D: Applied Physics*, 55(2):025201, 2021. doi:10.1088/1361-6463/ac2a76.
- [4] A. E. Guile, A. H. Hitchcock, K. Dimoff, and A. K. Vijh. Physical implications of an effective activation energy for arc erosion on oxidised cathodes. *Journal of Physics D: Applied Physics*, 15(11):2341, 1982. doi:10.1088/0022-3727/15/11/026.
- [5] P. Teste, T. Leblanc, and J. P. Chabrierie. Study of the arc root displacement and three-dimensional modelling of the thermal phenomena occurring in a hollow cathode submitted to an electric moving arc. *Journal of Physics D: Applied Physics*, 28(5):888–898, 1995. doi:10.1088/0022-3727/28/5/010.
- [6] A. Marotta and L. I. Sharakhovsky. A theoretical and experimental investigation of copper electrode erosion in electric arc heaters: I. the thermophysical model. *Journal of Physics D: Applied Physics*, 29(9):2395, 1996.
- [7] A. Monnoyer, P. Freton, and J. J. Gonzalez. Heat transfer in the solid cathode of a hollow cathode plasma torch. *Plasma Physics and Technology*, 10(2):94–98, 2023. doi:10.14311/ppt.2023.2.94.
- [8] L. I. Sharakhovsky, A. Marotta, and V. N. Borisyuk. A theoretical and experimental investigation of copper electrode erosion in electric arc heaters: II. the experimental determination of arc spot parameters. *Journal of Physics D: Applied Physics*, 30(14):2018, 1997. doi:10.1088/0022-3727/30/14/009.
- [9] R. Landfried, T. Leblanc, M. Kirkpatrick, and P. Teste. Assessment of the power balance at a copper cathode submitted to an electric arc by surface temperature measurements and numerical modelling. *IEEE Transactions on Plasma Science*, 40(4):1205–1216, 2012. doi:10.1109/TPS.2012.2185069.
- [10] S. Coulombe. *A model of the electric arc attachment on non-refractory (cold) cathodes*. PhD thesis, McGill University - Montréal, 1997.
- [11] B. Jüttner. Cathode spots of electric arcs. *Journal of Physics D: Applied Physics*, 34(17):R103, 2001. doi:10.1088/0022-3727/34/17/202.
- [12] V. Nemchinsky. Heat transfer to a cathode of a rotating arc. *Plasma Sources Science and Technology*, 24(3):035013, 2015. doi:10.1088/0963-0252/24/3/035013.
- [13] N. A. Almeida, M. S. Benilov, L. G. Benilova, et al. Near-cathode plasma layer on cu-cr contacts of vacuum arcs. *IEEE Transactions on Plasma Science*, 41(8):1938–1949, 2013. doi:10.1109/TPS.2013.2260832.
- [14] I. Beilis. *Plasma and spot phenomena in electrical arcs*, volume 113. Springer Nature, 2020.
- [15] M. S. Benilov. Understanding and modelling plasma-electrode interaction in high-pressure arc discharges: a review. *Journal of Physics D: Applied Physics*, 41(14):144001, 2008. doi:10.1088/0022-3727/41/14/144001.
- [16] M. S. Benilov, M. D. Cunha, W. Hartmann, et al. Space-resolved modeling of stationary spots on copper vacuum arc cathodes and on composite cu-cr cathodes with large grains. *IEEE Transactions on Plasma Science*, 41(8):1950–1958, 2013. doi:10.1109/TPS.2013.2263255.
- [17] M. S. Benilov. Maxwell's construction for non-linear heat structures and determination of radius of arc spots on cathodes. *Physica Scripta*, 58(4):383, 1998. doi:10.1088/0031-8949/58/4/015.
- [18] R. N. Szenté, R. J. Munz, and M. G. Drouet. The influence of the cathode surface on the movement of magnetically driven electric arcs. *Journal of Physics D: Applied Physics*, 23(9):1193, 1990. doi:10.1088/0022-3727/23/9/009.